[13] M. Maeda and A. Sumioka, "Computer-aided design of parametric amplifiers," *IEEE Trans. Microwave Theory and Tech. (1971 Symposium Issue)*, vol. MTT-19, pp. 916–921, Dec. 1971.
[14] H. C. Okean and H. Weingart, "S-band integrated parametric amplifier having both flat-gain and linear phase response, *IEEE Trans. Microwave Theory Tech. (1968 Symposium Issue)*, vol. MTT-16, pp. 1057–1059, Dec. 1968.
[15] H. Takahashi, "General theory of parametric amplifiers," presented at Symp., Session 8, Joint Conv. IEE, London, and IECE, Tokyo, Japan, 1959.
[16] J. Kliphuis, "C-band nondegenerate parametric amplifier with 500-Mc bandwidth," *Proc. IRE*, vol. 49, pp. 961, May 1961.
[17] S. Hayasi and T. Kurokawa, "A balanced-type parametric amplifier," *IRE Trans. Microwave Theory Tech.*, vol. MTT-10, pp. 185–190, May 1962.
[18] J. D. Pearson and K. S. Lunt, "A broadband balanced idler circuit for parametric amplifiers," *Radio Electron. Engr.*, pp. 331–333, May 1964.
[19] M. Grace, "An extremely wideband tunable *S*-band parameter amplifier," *Proc. IRE*, vol. 49, p. 1940, Dec. 1961.
[20] J. Edrich, "Low noise parametric natural resonance amplifiers with large bandwidths," *Frequenz*, pp. 337–343, May 20, 1966.
[21] A. H. Benny and J. Pearson, "A high-frequency wideband idler circuit for parametric amplifiers," *Proc. IEEE* (Corresp.), vol. 53 p. 181, Feb. 1965.
[22] H. Watson, *Microwave Semiconductor Devices and Their Circuit Applications*. New York: McGraw-Hill, 1969.
[23] W. J. Getsinger and G. L. Matthaei, "Some aspects of the design of wide-band up-converts and nondegenerate parametric amplifiers," *IEEE Trans. Microwave Theory Tech. (1963 Symposium Issue)*, vol. MTT-12, pp. 77–87, Jan. 1964.
[24] W. J. Getsinger, "Prototypes for use in broadbanding reflection. amplifiers," *IEEE Trans. on Microwave Theory Tech.*, vol. MTT-11, pp. 486–497, Nov. 1963.
[25] D. Wilde and C. Beighter, *Foundations of Optimization*, Englewood Cliffs, N. J.: Prentice-Hall, 1967.
[26] G. Temes and D. Calahan, "Computer-aided network optimization. The state-of-the-art," *Proc. IEEE (Special Issue on Computer-Aided Design)*, vol. 55, pp. 1832–1863, Nov. 1967.
[27] J. W. Bandler and P. A. MacDonald, "Optimization of microwave networks by razor search," *IEEE Trans. Microwave Theory Tech., (Special Issue on Computer-Oriented Microwave Practices)*, vol. MTT-17, pp. 552–562, Aug. 1969.
[28] G. L. Matthaei, L. Young, and E. M. T. Jones, *Microwave Filters, Impedance Matching Networks and Coupling Structures*. New York: McGraw-Hill, 1964.

An Octave-Band Switched-Line Microstrip 3-b Diode Phase Shifter

ROBERT P. COATS

***Abstract*—The design of an octave-band (2.5–5.0-GHz) switched-line diode phase shifter is described. An analysis showing the need for a choice of the shunt-diode switch configuration for broad-band operation is presented. Curves of even- and odd-mode impedance of parallel coupled microstrip lines employed in Schiffman differential phase shifters are presented. The configuration and performance characteristics of the phase shifter are described.**

I. Introduction

IN A RECENT PAPER [1], it was concluded that microwave switched-line diode phase shifters employing coupled transmission-line elements of the type described by Schiffman [2] were limited in bandwidth to about 1/2 octave. It was further stated that this bandwidth limitation occurs because the effective length of the off transmission path becomes a multiple of a half-wavelength in the frequency band of interest, where all incident power is reflected back to the generator.

In this paper, the off-path insertion loss of switched-line phase shifters employing both series- and shunt-configured diode switches is determined. It is shown that the bandwidth limitation described in [1] can be averted by use of the shunt configuration. The design of an octave-band switched-line 3-b microstrip diode phase shifter operating in the 2.5–5.0-GHz frequency band is presented. The performance characteristics of this phase shifter are also included.

Manuscript received September 21, 1972; revised January 12, 1973.
The author is with the Antenna and Microwave Systems Branch, Texas Instruments, Incorporated, Dallas, Tex. 75222.

II. Effect of Switch Configuration on Phase-Shifter Performance

The two configurations that were considered for the phase shifter to be described are shown in Fig. 1. The configuration utilizing series diode switches was initially thought to be the most desirable because the position of the diodes relative to the input and output junctions does not impose a potential bandwidth limitation as it does in the shunt-diode switch case. However, analysis of a mathematical model of the configuration utilizing series switches revealed that it had operating points in the octave band at which the isolation between switching paths becomes very low. At these points, the phase-shifter insertion loss becomes very high and the phase error large. The configuration employing shunt diode switches was not found to have this problem. The problem was examined further by determining the insertion loss of the off transmission path (i.e., the path where maximum insertion loss is desired) [3]. The problem under consideration exists when some separation of good quality diodes is found to produce very low insertion loss in that path. This analysis is initiated by considering the two-port network having wave amplitudes a_1 and b_1 at port 1 and a_2 and b_2 at port 2, as shown in Fig. 2. The wave amplitudes at port 1 and port 2 are related using the cascading matrix T:

$$\begin{bmatrix} b_1 \\ a_1 \end{bmatrix} = T \begin{bmatrix} a_2 \\ b_2 \end{bmatrix} = \begin{bmatrix} t_{11} & t_{12} \\ t_{21} & t_{22} \end{bmatrix} \begin{bmatrix} a_2 \\ b_2 \end{bmatrix}. \quad (1)$$

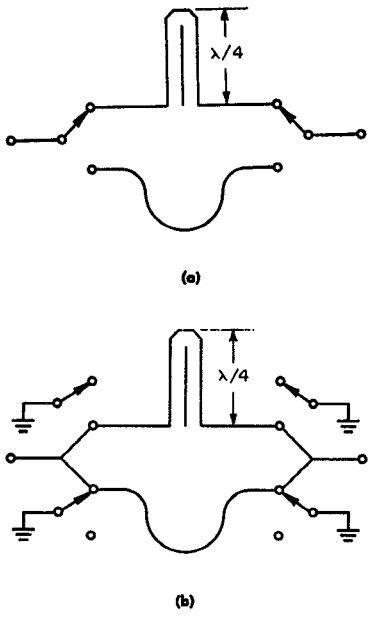

Fig. 1. Configuration of phase-shifter bits considered. (a) Series diode switch configuration. (b) Shunt diode switch configuration.

Fig. 2. Network model.

The insertion loss of the network is determined by expanding this equation and assuming the output is terminated in a matched load (i.e., $a_2=0$):

$$b_1 = t_{12}b_2 \tag{2}$$

$$a_1 = t_{22}b_2 \tag{3}$$

$$b_2/a_1 = 1/t_{22} \tag{4}$$

$$L = \text{insertion loss} = 20\log_{10}\left|\, b_2/a_1 \,\right| = 20\log_{10}\left|\, 1/t_{22} \,\right| . \tag{5}$$

The circuits to be considered and the cascading matrices required are shown in Fig. 3 [4]. For a single-element diode switch, the insertion loss is obtained using the T_1 matrix for each switch configuration. For the series configuration this loss in decibels becomes

$$L_{\text{series}} = 20\log_{10}\left|\frac{2}{Z/Z_0 + 2}\right| \tag{6}$$

and for the shunt configuration it is

$$L_{\text{shunt}} = 20\log_{10}\left|\frac{2}{Y/Y_0 + 2}\right| . \tag{7}$$

For the composite circuits shown, the cascading matrix is

$$T_T = T_1T_2T_3 \tag{8}$$

and the insertion loss is found by using the element t_{22} of this matrix in (5). When the matrix multiplication is carried out, the insertion losses of the circuits of Fig. 3(a) and (b) are found to be

$$L_{\text{series}} = 20\log_{10}\left|\frac{4e^{j\theta}}{-(Z/Z_0)^2 + (Z/Z_0 + 2)^2e^{j2\theta}}\right| \tag{9}$$

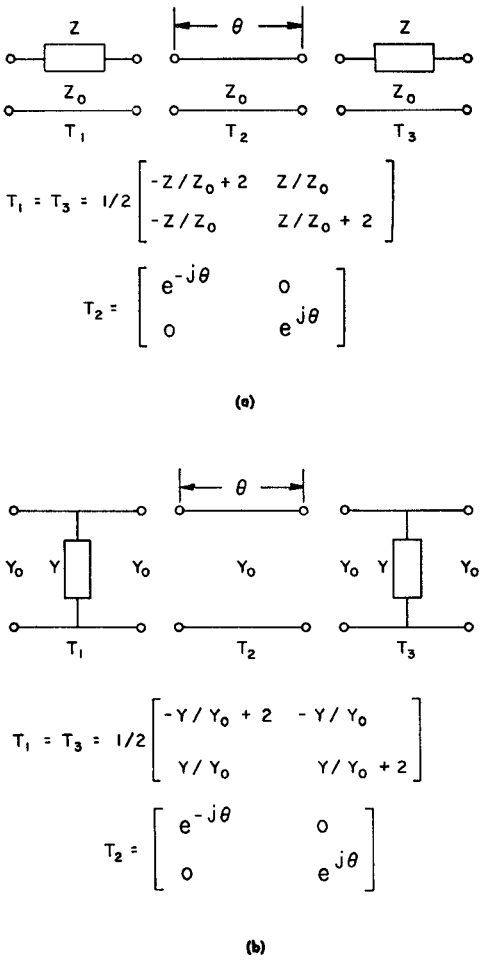

Fig. 3. Diode switch circuits and the cascading matrices of elements. (a) Series switch. (b) Shunt switch.

and

$$L_{\text{shunt}} = 20\log_{10}\left|\frac{4e^{j\theta}}{-(Y/Y_0)^2 + (Y/Y_0 + 2)^2e^{j2\theta}}\right| . \tag{10}$$

A. Zero Parasitic Reactance

If we neglect parasitic reactances associated with the diode configuration and its mounting, the diode element values required for the transmission-path open condition become

$$Z = -jX, \qquad \text{for the series case}$$

and

$$Y = 1/R, \qquad \text{for the shunt case.}$$

Substituting these into (9) and (10) we have

$$L_{\text{series}} = 20\log_{10}\left|\frac{4e^{j\theta}}{(X/Z_0)^2 + [(X/Z_0)^2 + 4]e^{j(2\theta - 2\tan^{-1}X/2Z_0)}}\right| \tag{11}$$

and

$$L_{\text{shunt}} = 20\log_{10}\left|\frac{4e^{j\theta}}{-(Z_0/R)^2 + (Z_0/R + 2)^2e^{j2\theta}}\right| . \tag{12}$$

From (11) it is seen that zero insertion loss or isolation occurs for the series switch when

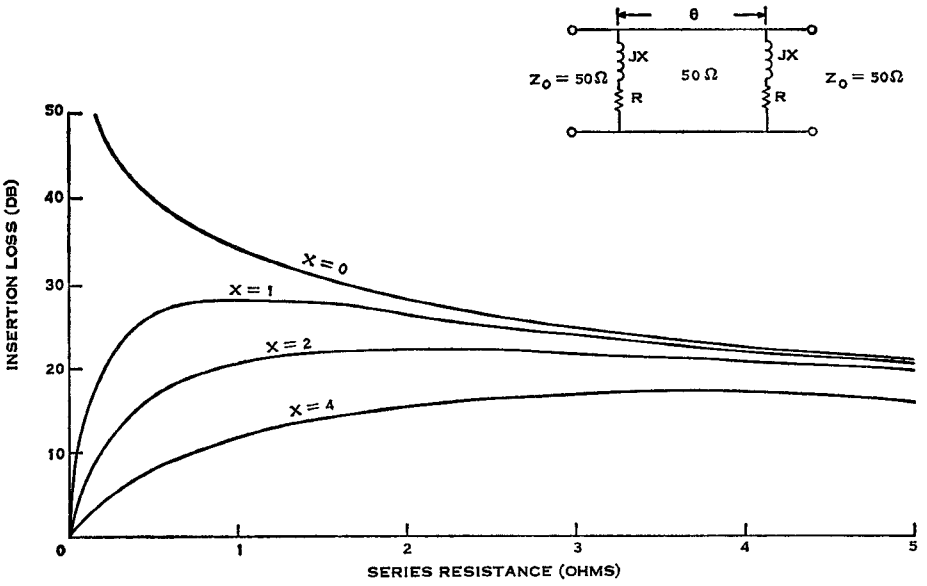

Fig. 4. Minimum phase-shifter off-path insertion loss as a function of diode real and imaginary impedance.

$$2\theta - 2\tan^{-1} X/2Z_0 = (2m + 1)180, \qquad m = 0, 1, 2, 3, \cdots$$

or

$$\theta = \tan^{-1} X/2Z_0 + (2m + 1)90, \qquad m = 0, 1, 2, 3, \cdots. \quad (13)$$

For the shunt switch, a minimum value of insertion loss occurs when

$$2\theta = m360, \qquad m = 0, 1, 2, 3, \cdots$$

or

$$\theta = m180, \qquad m = 0, 1, 2, 3, \cdots. \quad (14)$$

At this point, the shunt-switch isolation becomes

$$L_{\text{shunt}} = 20 \log_{10} \left| \frac{1}{Z_0/R + 1} \right|. \quad (15)$$

In order for the designer to make use of the series switch, it is necessary to space the diodes close enough together to prevent θ from reaching the value of (13) in the band of interest. If the designer expects to obtain 20-dB insertion loss from a single diode, he finds the X/Z_0 required from (6) to be 19.9. Substituting this into (13) gives a separation for zero insertion loss of

$$\theta = 84.3 + (2m + 1)90, \qquad m = 0, 1, 2, 3, \cdots$$

or

$$\theta = 174.3^0, 354.3^0, 534.3^0, \cdots$$

when two diodes of this quality are used. From these results it is seen that use of the series switch for the octave-band Schiffman differential phase shifter is impractical; there is not sufficient separation between minimum isolation points to permit octave-band operation between them, and the length of the coupled-line element is too long (180° at center frequency) to permit operation below the smallest diode separation giving zero isolation.

These problems are not encountered with the shunt switch. A shunt-mounted diode can be found to provide a Z_0/R of approximately 50 when operated in a 50-Ω microstrip transmission line. With this Z_0/R ratio, a single diode is found from (7) to provide 28.3-dB isolation, and two diodes spaced 180° apart to provide minimum isolation are found from (15) to provide 34.1-dB isolation.

It is seen that when two cascaded diode switches are utilized, minimum values of isolation occur when the diodes are spaced at approximate multiples of $\lambda/2$. The actual spacing for series switches depends upon the X/Z_0 ratio, but for good quality diodes it is close to $\lambda/2$. For shunt switches it is exactly $\lambda/2$. For series switches, the isolation reduces to zero at these points. For shunt switches, the isolation is approximately 6 dB greater than that obtainable with a single diode.

B. Finite Parasitic Reactance

It is now clear that the shunt diode configuration is superior to the series configuration when utilized for broad-band switched-line phase-shifter applications. However, the off-path insertion loss obtainable with the shunt diode configuration can be severely degraded by parasitic reactance associated with the diode package and its mounting. Performance degradation caused by large-series equivalent parasitic inductance is probably the most common encountered by designers. This degradation can be analyzed by allowing the diode element values required for the transmission-path open condition in (10) to become

$$Y = 1/(R + jX) \quad (16)$$

where jX is the series equivalent inductive reactance of the diode. When this is done, (10) becomes

$$L_{\text{shunt}} = \left| \frac{4e^{j\theta}}{-[Z_0/(R+jX)]^2 + [Z_0/(R+jX) + 2]^2 e^{j2\theta}} \right|. \quad (17)$$

Equation (17) can be shown to have a minimum value when

$$\theta = \tan^{-1} Z_0X/(RZ_0 + 2R^2 + 2X^2) - \tan^{-1} X/R + m180, \qquad m = 1, 2, 3, \cdots. \quad (18)$$

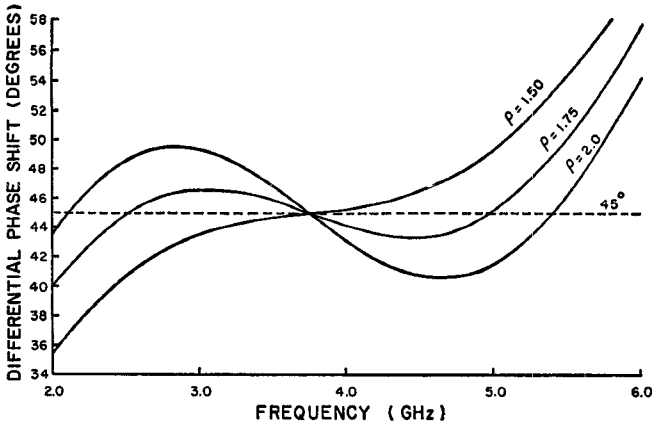

Fig. 5. Theoretical performance of 45° Shiffman phase shifter.

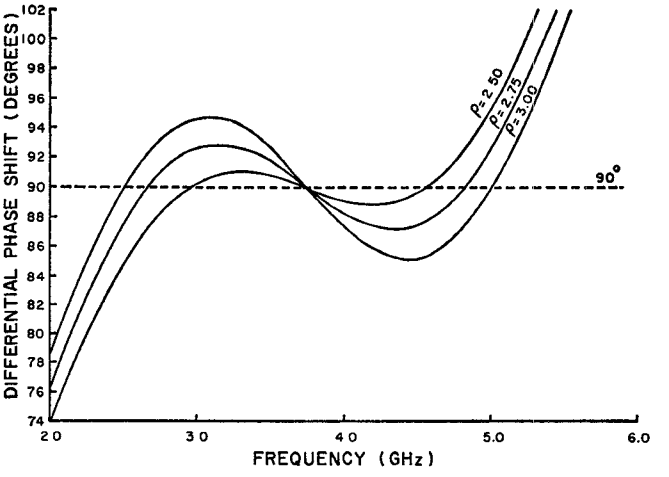

Fig. 6. Theoretical performance of 90° Shiffman phase shifter.

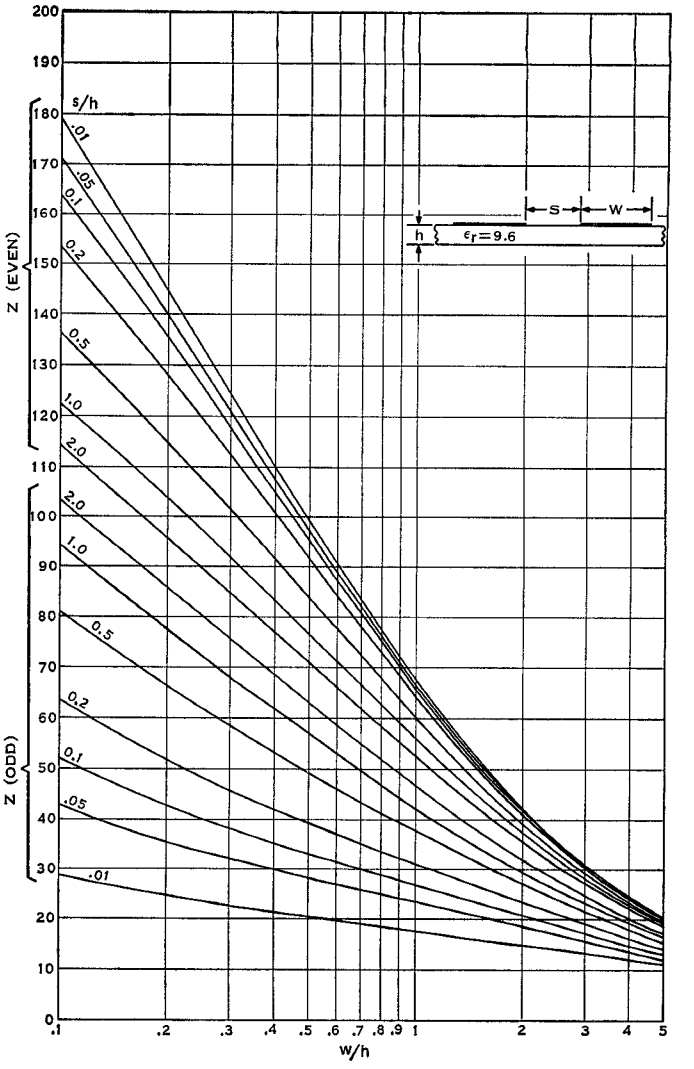

Fig. 7. Even- and odd-mode characteristic impedance for coupled microstrip transmission lines.

At this point, the off-path insertion loss becomes

$$L_{\text{shunt}} = 20 \log_{10} \cdot \left| \frac{4(R^2+X^2)^2}{-Z_0^2(R^2+X^2)+[(RZ_0+2R^2+2X^2)^2+(Z_0X)^2]} \right| . \quad (19)$$

This minimum insertion loss is shown for a 50-Ω characteristic impedance environment as a function of diode real and imaginary impedance in Fig. 4. For the case of zero parasitic inductance, the insertion loss is limited only by the minimum value of diode resistance available. For cases of finite parasitic inductance, a reduction in diode resistance may result in lower insertion loss unless an accompanying reduction in inductance is made. For the limiting case where the diode resistance becomes zero, the values of minimum insertion loss become zero, as in the case employing series diodes.

III. Phase-Shifter Design and Performance

After performing the foregoing analysis to determine the switch configuration required to achieve broad-band performance, a switched-line phase shifter utilizing a microstrip transmission line was designed to operate in the 2.5–5.0-GHz frequency band. It was constructed on 0.020-in thick 99.5-percent aluminum oxide substrate material, and utilized parallel-coupled transmission lines one-quarter wavelength long at center band to form Schiffman-type differential phase shifters of 45, 90, and 180°. From [2], the theoretical performances of Schiffman 45 and 90° phase shifters were determined for three values of the even- to odd-mode impedance ratio ρ. These calculated performance curves are shown in Figs. 5 and 6. From these it is seen that the values of ρ required to obtain equal ripple phase error are 1.75 and 2.75 for the 45 and 90° bits, respectively. Two coupled lines of the type employed in the 90° bit were used in the 180° bit. All coupled lines were designed using the curves of even- and odd-mode impedance versus geometry shown in Fig. 7. These curves were derived using the MAXCAP 10 [5] computer program which makes use of Green's functions to determine the charge distribution on the strip-conductor system employed. From the charge distributions, the elements of the Maxwellian capacitance matrix are determined, and from these elements, the even- and odd-mode impedances are determined.

With the coupled-line configurations determined, the major design task remaining was that of determining the form of the input/output circuit used in each bit. These circuits must provide an adequate impedance match when energy is switched to either the uniform or coupled transmission-line paths, an adequate dc isolation between diodes in the two

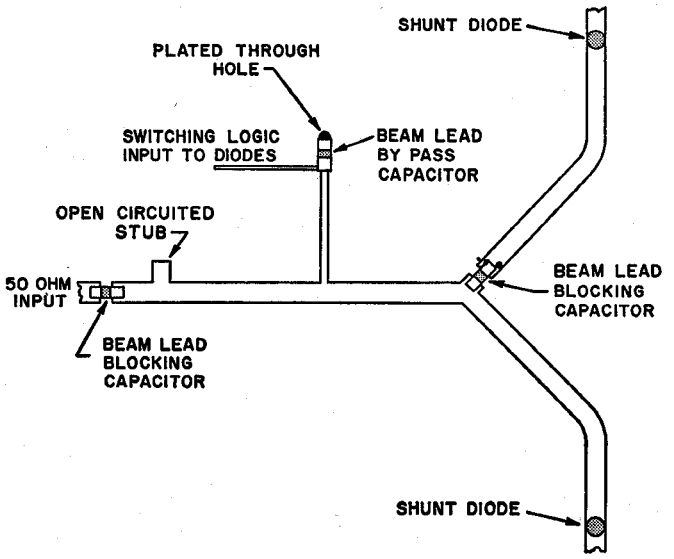

Fig. 8. Input/output circuit configuration used in phase shifter.

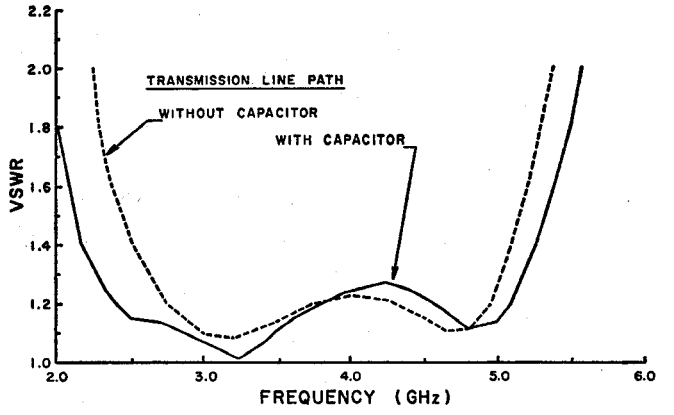

Fig. 9. Calculated performance of phase-shifter input/output circuit.

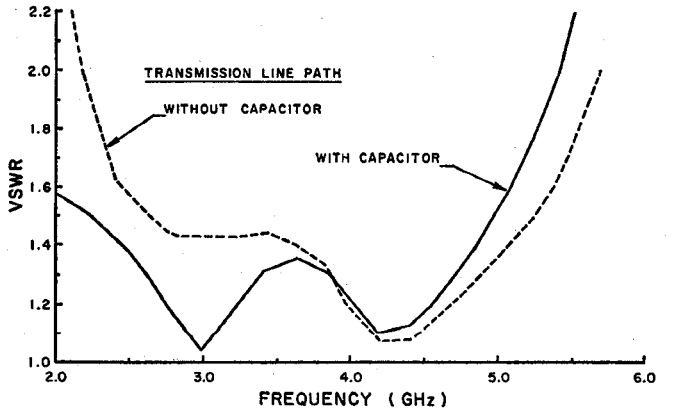

Fig. 10. Measured performance of phase-shifter input/output circuit.

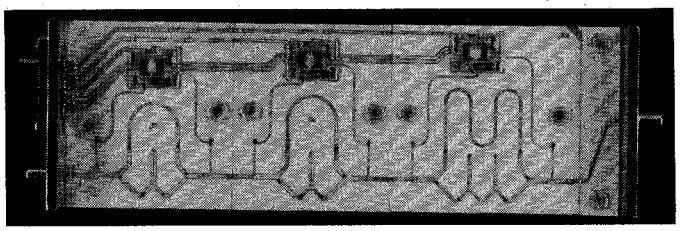

Fig. 11. Photograph of the octave-band 3-b phase shifter.

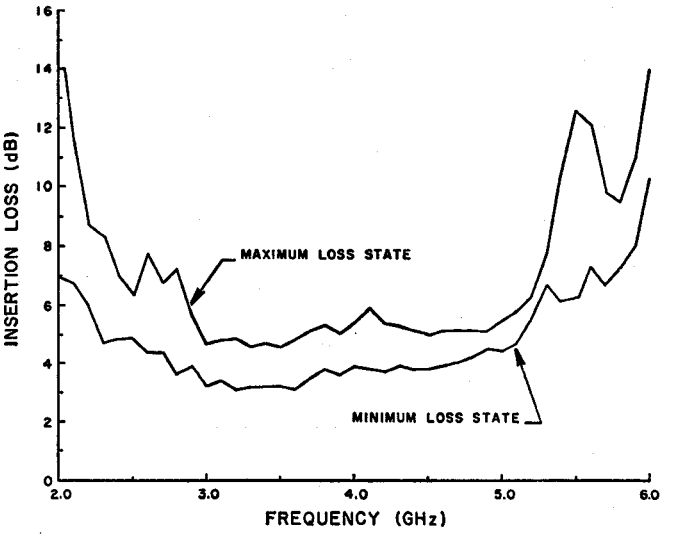

Fig. 12. Measured insertion loss versus frequency of typical phase shifter.

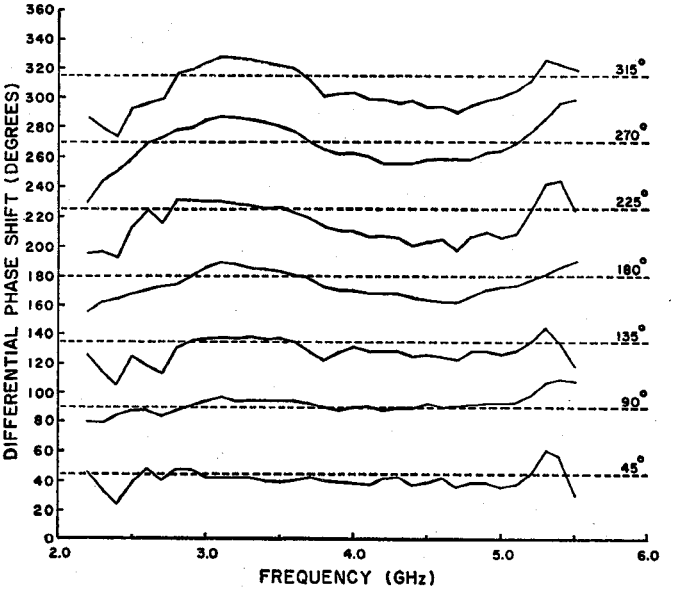

Fig. 13. Measured differential phase shift versus frequency of typical phase shifter.

transmission paths, and an adequate isolation between the RF and diode-switching logic circuits. The form of the circuit developed is shown in Fig. 8. A shorted stub for matching purposes is achieved by connecting a stub to a plated-through hole via a 12-pF beam-lead capacitor. Diode switching is accomplished by attaching the driver output to the stub end of this capacitor. Diode switching paths are isolated by use of 5-pF beam-lead blocking capacitors located near Wye-junction centers. This circuit configuration was optimized by using the CAIN 02 computer program [6]. This is a generalized routine for computer-aided design of linear time-invariant electronic circuits. The predicted voltage standing-wave ratio (VSWR) provided by CAIN 02 is shown in Fig. 9 and the measured VSWR is shown in Fig. 10. Improvement in the-

oretical performance was limited by the space available for tuning elements. Differences between predicted and measured performance are attributed primarily to errors in the lumped-element equivalent-circuit representations of diodes and capacitors.

The diodes employed are Hewlett-Packard 5082–3258 high-speed p-i-n diodes. The diode driver is a thick-film hybrid microcircuit designed to provide a two-phase high-current output from a single-phase emitter-coupled logic (ECL) input. It is basically a p-n-p emitter-coupled amplifier and phase-shifter stage driving a balanced emitter-coupled n-p-n output stage. It provides 10 mA to each of two ON diodes, while reverse biasing the two OFF diodes to 2 V. The desired throughput time of 5–10 ns is achieved by using high-peak reverse current, low resistance values, and emitter speed-up capacitance in the output stage. The total time required to change phase-shifter states is approximately 12–15 ns.

A photograph of the complete 3-b phase-shifter assembly is shown in Fig. 11. Sixty of these units have been built and evaluated for use in a phased-array antenna application. Performance characteristics of a typical unit are shown in Figs. 12 and 13. Fig. 12 shows the limits of insertion loss incurred as the phase shifter is switched through all eight switching states. Fig. 13 shows the differential phase shift provided as the phase shifter is switched from the reference state or transmission path void of coupled transmission lines to the remaining seven phase states. Phase errors that are significantly larger than that theoretically predicted using the curves of Figs. 5 and 6 are due to improper complementary transmission-line length and impedance mismatches in coupled sections and input/output Wye junctions. The divergence between minimum and maximum insertion loss shown in Fig. 12 is also caused by these impedance mismatches.

IV. Conclusions

Switched-line diode phase shifters employing Schiffman differential phase elements can provide bandwidths in excess of an octave if the proper diode switch configuration is employed. Low phase errors can be achieved over this band with single-section coupling sections if proper care is taken to limit internal reflections caused by impedance mismatches. In the phase shifter described herein, designated elements in each bit were individually optimized. Better performance can be realized by using a computer-aided design technique to perform this optimization on a mathematical-model representation of the composite 3-b phase-shifter system.

References

[1] R. V. Garver, "Broad-band diode phase shifters," *IEEE Trans. Microwave Theory Tech.*, vol. MTT-20, pp. 314–323, May 1972.
[2] B. M. Schiffman, "A new class of broad-band microwave 90-degree phase shifters," *IRE Trans. Microwave Theory Tech.*, vol. MTT-6, pp. 232–237, Apr. 1958.
[3] R. P. Coats, "Use of diode switches in broadband diode phase shifter applications," Texas Instruments, Inc., Dallas, unpublished Memo., Dec. 1970.
[4] D. M. Kerns and R. W. Beatty, *Basic Theory of Waveguide Junctions and Introductory Microwave Network Analysis*. Oxford, England: Pergamon Press, 1967.
[5] R. A. Zachary, Jr., and L. W. Dyer, "Maxwellian capacitance matrix for a system of parallel strip conductors on a dielectric interface," Design Automation Dep., Texas Instruments, Inc., Dallas, unpublished Tech. Memo., Dec. 1967.
[6] T. W. Houston, L. W. Dyer, and G. J. Policky, "Computer-aided design of microwave integrated circuits," in *IEEE Wescon Conv. Rec.*, pt. 2, session 6, Aug. 1969.